Articles

Synthesis and Thermal Behavior of Novel Si−B−C−N Ceramic Precursors

Markus Weinmann,*,† Jörg Schuhmacher,‡ Horst Kummer,† Sabine Prinz,† Jianqiang Peng,† Hans Jürgen Seifert,† Martin Christ,† Klaus Müller,‡ Joachim Bill,† and Fritz Aldinger†

Max-Planck-Institut für Metallforschung and Institut für Nichtmetallische Anorganische Materialien, Pulvermetallurgisches Laboratorium, Universität Stuttgart, Heisenbergstrasse 5, D-70569 Stuttgart, Germany, and Physikalisch-Chemisches Institut, Universität Stuttgart, Pfaffenwaldring 55, D-70569 Stuttgart, Germany

Received March 11, 1999. Revised Manuscript Received November 18, 1999

Several boron-modified polysilazanes of general type $\{B[C_2H_4Si(R)NH]_3\}_n$ ($C_2H_4 = CHCH_3$ or CH_2CH_2) were synthesized and their thermal behavior studied. In contrast to the known derivatives with R = alkyl or aryl, we describe ceramic precursors in which the bulky moieties R are substituted with lower weight groups and/or reactive entities. Reactive units enable further cross-linking of the polymeric framework and therefore minimize depolymerization during ceramization. The polymer-to-ceramic conversion of all synthesized polymers was monitored by thermogravimetric analysis. Both low molecular weight substituents and/or cross-linking units increase the ceramic yield from 50% ($R = CH_3$) to 83−88%. High-temperature thermogravimetric analysis in an inert gas atmosphere indicates the ceramics obtained are stable up to ∼2000 °C. XRD studies of the fully amorphous materials point out that, with increasing temperature, formation of α-SiC or α-SiC/β-Si_3N_4 crystalline phases occurs at 1550−1750 °C, depending on the material's composition. The resistance of these novel materials toward oxidative attack was investigated by TGA in air up to 1700 °C and SEM/EDX, indicating that the materials efficiently self-protect toward oxidation.

1. Introduction

Organometallic polymers containing the elements silicon, boron, carbon, nitrogen, and hydrogen are precursors for silicon nitride-, silicon carbide-, and boron nitride-based Si−B−C−N ceramics.[1−3] Their extraordinary high-temperature stability, coupled with a high resistance toward oxidation, has prompted considerable interest in these new materials.[2−7]

First described by Seyferth et al. in 1990, silazanes were reacted with borane dimethyl sulfide to obtain silazane-substituted borazines.[8] Structurally comparable borazine-based Si−B−C−N polymers were also described by Sneddon et al. who reacted borazine via thermal dehydrocoupling with oligo- or polysilazanes.[9] Recently, Paine et al.[10] published a method for synthesizing borazine-based Si−B−C−N polymers by reacting B-chloroborazines with $LiSi[Si(CH_3)_3]_3$ followed by subsequent polymerization with hexamethyldisilazane.

Aminolysis of $Cl_3SiNHBCl_2$ (TADB) with methylamine as described by Baldus and Jansen produces

* To whom correspondence should be addressed. E-mail: weinmann@aldix.mpi-stuttgart.mpg.de.
† Max-Planck-Institut für Metallforschung and Institut für Nichtmetallische Anorganische Materialien.
‡ Physikalisch-Chemisches Institut.

(1) (a) Birot, M.; Pillot, J.-P.; Dunogués, J. *Chem. Rev.* **1995**, *95*, 1443 and references therein. (b) Toreki, W. *Polym. News* **1991**, *16*, 1.
(2) (a) Bill, J.; Aldinger, F. *Adv. Mater.* **1995**, *7*, 775. (b) Bill, J.; Aldinger, F. *Z. Metallkd.* **1996**, *87*, 827.
(3) Baldus, H.-P.; Jansen, M. *Angew. Chem.* **1997**, *109*, 338; *Angew. Chem., Int. Ed. Engl.* **1997**, *36*, 328.
(4) Takamizawa, M.; Kobayashi, T.; Hayashida, A.; Takeda, Y. US Patent 4, 604,367, 1986.
(5) Baldus, H.-P.; Jansen, M.; Wagner, O. *Key Eng. Mater.* **1994**, *89−91*, 75.
(6) Riedel, R.; Kienzle, A.; Dressler, W.; Ruwisch, L. M.; Bill, J.; Aldinger, F. *Nature* **1996**, *382*, 796.
(7) (a) Heimann, D.; Bill, J.; Aldinger, F. Fortschrittsberichte der Deutschen Keramischen Gesellschaft, Werkstoffe-Verfahren-Anwendungen, Board 10, Keramische Schichten, 1995 (in German). (b) Heimann, D. Ph.D. Thesis, Universität Stuttgart, 1996 (in German).
(8) (a) Seyferth, D.; Plenio, H. *J. Am. Ceram. Soc.* **1990**, *73*, 2131. (b) Seyferth, D.; Plenio, H.; Rees, W. S., Jr.; Büchner, K. In *Frontiers of Organosilicon Chemistry*, Bassindale, A. R., Gaspar, P. P., Eds.; Royal Society of Chemistry: Cambridge 1991; p 15.
(9) (a) Su, K.; Remsen, E. E.; Zank, G. A.; Sneddon, L. G. *Chem. Mater.* **1993**, *5*, 547. (b) Su, K.; Remsen, E. E.; Zank, G. A.; Sneddon, L. G. *Polym. Prepr.* **1993**, *34*, 334. (c) Wideman, T.; Su, K.; Remsen, E. E.; Zank, G. A.; Sneddon, L. G. *Chem. Mater.* **1995**, *7*, 2203. (d) Fazon, P. J.; Remsen, E. E.; Beck, J. S.; Carroll, P. J.; McGhie, A. R.; Sneddon, L. G. *Chem. Mater.* **1995**, *7*, 1942. (e) Wideman, T.; Su, K.; Remsen, E. E.; Zank, G. A.; Sneddon, L. G. *Mater. Res. Soc. Symp. Proc.* **1996**, *410*, 185. (f) Wideman, T. T.; Cortez, E.; Remsen, E. E.; Zank, G. A.; Carroll, P. J.; Sneddon, L. G. *Chem. Mater.* **1997**, *9*, 2218.
(10) Srivastava D.; Duesler, E. N.; Paine, R. T. *Eur. J. Inorg. Chem.* **1998**, 855.

10.1021/cm9910299 CCC: $19.00
Published on Web 02/08/2000

N-methylpolyborosilazane.[3,5,11] This precursor has already been used successfully for the production of Si−B−C−N ceramic fibers with remarkable high-temperature mechanical properties.[3] An alternative single source precursor, promising for the production of bulk ceramic material, can be prepared by ammonolysis of $B[C_2H_4Si(CH_3)Cl_2]_3$ as described by Kienzle and Riedel et al.[12,13] Ceramics derived from this precursor are stable for a limited time at temperatures of more than 2000 °C.[6] The latest publications of Riedel describe the synthesis of polymers with increased boron contents using $HBCl_2{\cdot}SMe_2$ or $H_2BCl{\cdot}SMe_2$ instead of a $BH_3{\cdot}SMe_2$.[14] Alternative, higher boron contents in boron modified polysilazanes can also be obtained by hydroboration with dialkylboranes as described by Matsumoto et al.[15]

Recently we described the synthesis of Si−B−C−N polymers using an oxide-free sol−gel process. Boron-modified polysilylcarbodi-imides were obtained from $B[C_2H_4Si(R)Cl_2]_3$ (R = H, CH_3, Cl) and $Me_3Si{-}N{=}C{=}N{-}SiMe_3$.[16,17] Finally, Si−B−C−N polymers have also been obtained by hydrosilylating vinyl-substituted polysilazanes with $B[C_2H_4Si(R)H_2]_3$.[18] This reaction requires neither solvents nor catalysts and produces no byproducts.

The precursors enumerated above are usually transformed into ceramics by thermolysis in inert gas atmospheres. This polymer-to-ceramic conversion is always accompanied by the formation of gaseous species. Consequently, dense polymer-derived bulk ceramics without open pores are difficult to obtain. The accompanying shrinkage that takes place during thermolysis frequently causes cracks, in the worst case destroying bulk parts.[3,17] Thus, polymeric precursor design is an important issue in that mass loss during thermolysis must be kept as low as possible, while maintaining good processability, controlled reactivity, and low cost. In this paper we focus mainly on developing novel precursors obtained by simple reactions which deliver high-temperature-stable ceramics in high ceramic yields.

2. Experimental Section

2.1. General Comments. All reactions were carried out in a purified argon atmosphere using standard Schlenk techniques.[19] The syntheses of the poly(vinylsilazane)s $[(H_2C{=}CH)Si(R)NH]_n$ [R = H,[20] $(NH)_{0.5}$[21]] as well as the tris(chlorosilylethyl)boranes $B[C_2H_4Si(R)Cl_2]_3\}_n$ (R = H,[16a] Cl[22]) were performed according to procedures described in the literature. Chlorovinylsilanes used were obtained from ABCR chemicals and freshly distilled from magnesium. $LiAlH_4$ powder (95%) was achieved from Merck AG. Borane dimethyl sulfide (2 M solution in toluene) was obtained from Sigma Aldrich. Diethyl ether was purified by distillation from CaH_2; tetrahydrofuran and toluene were purified by distillation from potassium.

Fourier transform infrared spectra were obtained with a Bruker IFS66 spectrometer in a KBr matrix. Solid-state NMR experiments were performed on a Bruker CXP 300 or a Bruker MSL 300 spectrometer operating at a static magnetic field of 7.05 T (^{1}H frequency 300.13 MHz) using a 4 mm magic angle spinning (MAS) probe. ^{29}Si and ^{13}C NMR spectra were recorded at 59.60 and 75.47 MHz using the cross-polarization (CP) technique in which a spin lock field of 62.5 kHz and a contact time of 3 ms were applied. Typical recycle delays were 6−8 s. All spectra were acquired using the MAS technique with a sample rotation frequency of 5 kHz. ^{29}Si and ^{13}C chemical shifts were determined relative to external standard Q_8M_8, the trimethylsilyl ester of octameric silicate, and adamantane. These values were then expressed relative to the reference compound TMS (0 ppm). Microanalysis was performed using a combination of different equipment (ELEMENTAR Vario EL, ELTRA CS 800 C/S Determinator, LECO TC-436 N/O Determinator) and by atom emission spectrometry (ISA JOBIN YVON JY70 Plus). Thermogravimetric analysis (TGA) of the polymer-to-ceramic conversion was carried out in flowing argon atmosphere (50 cm^3/min) with Netzsch STA 409 (25−1100 °C; with a heating rate 2 °C/min) equipment in alumina crucibles. Bulk ceramization of preceramic material occurred in alumina Schlenk tubes in flowing argon at 25−1400 °C, with a heating rate 1 °C/min and a dwell time of 3 h. High-temperature TGA of the as-obtained ceramic samples operating Netzsch STA 501 equipment was carried out in argon atmosphere (25−2200 °C; heating rate (T < 1400 °C) 5 °C/min, (T > 1400 °C) 2 °C/min) using carbon crucibles. High-temperature TGA in air (25−1700 °C; heating rate 5 °C/min) was performed using alumina crucibles. The crystallization of as-obtained amorphous ceramics was investigated in graphite furnaces using graphite crucibles at 1400 and 1500−2000 °C (each 50 °C steps; heating rate (T < 1400 °C) 10 °C/min, (T > 1400 °C) 2 °C/min). The X-ray diffraction unit used for the structural investigations of the annealed samples was a Siemens D5000/Kristalloflex (Cu Kα1 radiation), equipped with an OED and a quartz primary monochromator. Finally, SEM and EDX investigations were performed with field emission equipment, ZEISS DSM982 Gemini with a Schottky field emitter.

2.2. Synthesis of $\{B[C_2H_4Si(H)NH]_3\}_n$ (1*M*). In a 4 L Schlenk flask, equipped with a gas inlet tube, a mechanical

(11) (a) Jansen, M.; Baldus, H.-P. Ger. Offen. DE 410 71 08 A1, 1992. (b) Baldus, H.-P.; Wagner, O.; Jansen, M. *Mater. Res. Soc. Symp. Proc.* **1992**, *271*, 821. (c) Jansen, M. *Solid State Ionics* **1998**, *101−103*, 1.

(12) (a) Kienzle, A. Diploma thesis, Univeristät Stuttgart, 1991. (b) Kienzle, A. Ph.D. Thesis, Universität Stuttgart, 1994.

(13) (a) Riedel, R.; Kienzle, A.; Petzow, G.; Brück, M.; Vaahs, T. Ger. Offen. DE 432 07 83 A1, 1994. (b) Riedel, R.; Kienzle, A.; Petzow, G.; Brück, M.; Vaahs, T. Ger. Offen. DE 432 07 84 A1, 1994. (c) Bill, J.; Kienzle, A.; Sasaki, M.; Riedel, R.; Aldinger, F. In *Ceramics: Charting the Future*; Vincenzini, P., Ed.; Techna Sri, 1995. (d) Riedel, R.; Bill, J.; Kienzle, A. *Appl. Organomet. Chem.* **1996**, *10*, 241.

(14) (a) Ruwisch, L. M.; Dressler, W.; Reichert, S.; Riedel, R. In *Organosilicon Chemistry III, From Molecules to Materials*; Auner, N., Weis, J., Eds.; Wiley-VCH: Weinheim, 1997; p 628. (b) Ruwisch, L. M.; Riedel, R. *Electrochem. Soc. Proc.* **1997**, *97−39*, 355. (c) Ruwisch, L. M. Ph.D. Thesis, Technische Universität Darmstadt, 1998. (d) Riedel, R.; Ruwisch, L. M.; An, L.; Raj, R. *J. Am. Ceram. Soc.* **1998**, *81*, 3341.

(15) (a) Matsumoto, R. L.; Schwark, J. M. U.S. Patent 5,206,327, 1993. (b) Matsumoto, R. L.; Schwark, J. M. U. S. Patent 5,386,006, 1995.

(16) (a) Weinmann, M.; Haug, R.; Bill, J.; Aldinger, F.; Schuhmacher, J.; Müller, K. *J. Organomet. Chem.* **1997**, *541*, 345. (b) Weinmann, M. In *Grain Boundary Dynamics of Precursor Derived Ceramics*; Bill, J., Wakai, F., Aldinger, F., Eds.; Wiley-VCH: Weinheim, 1999; p 83.

(17) (a) Weinmann, M.; Haug, R.; Bill, J.; De Guire, M.; Aldinger, F. *Appl. Organomet. Chem.* **1998**, *12*, 725. (b) Haug, R.; Weinmann, M.; Bill, J.; Aldinger, F. *J. Eur. Ceram. Soc.* **1999**, *19*, 1.

(18) (a) Kamphowe, T. W.; Weinmann, M.; Bill, J.; Aldinger, F. *Sil. Ind.* **1998**, *63*, 159. (b) Weinmann, M.; Kamphowe, T. W.; Bill, J.; Aldinger, F. Ger. Offen. DE 197 41 460 A1, 1999. (c) Kamphowe, T. W.; Weinmann, M.; Aldinger, F.; Schuhmacher, J.; Müller, K. Submitted to *Chem. Mater.*

(19) This preparative method is based on experiments developed by the German chemist Wilhelm Schlenk. All apparatuses are equipped with sidearms for pumping out the air and moisture and introducing inert gas. See also: Shriver, D. F.; Drezdzon, M. A. *The Manipulation of Air-Sensitive Compounds*, 2nd ed.; Wiley: New York, 1986.

(20) (a) Lavedrine, A.; Bahloul, D.; Goursat, P.; Choong Kwet Yive, N. S.; Corriu, R. J.; Leclerq, D.; Mutin, P. H.; Vioux, A. *J. Eur. Ceram. Soc.* **1991**, *8*, 221. (b) Choong Kwet Yive, N. S.; Corriu, R. J.; Leclerq, D.; Mutin, P. H.; Vioux, A. *New J. Chem.* **1991**, *15*, 85. (c) Choong Kwet Yive, N. S.; Corriu, R. J.; Leclerq, D.; Mutin, P. H.; Vioux, A. *Chem. Mater.* **1992**, *4*, 141. (d) Bahloul, D.; Pereira, M.; Goursat, P.; Choong Kwet Yive, N. S.; Corriu, R. J. *J. Am. Ceram. Soc.* **1993**, *76*, 1156. (e) Bahloul, D.; Pereira, M.; Goursat, P. *J. Am. Ceram. Soc.* **1993**, *76*, 1163.

(21) (a) Peuckert, M.; Vaahs, T.; Brück, M. *Adv. Mater.* **1990**, *2*, 398. (b) Huggins, J. Ger. Offen. DE 411 42 17 A1, 1992.

(22) Jones, P. R.; Myers, J. K. *J. Organomet. Chem.* **1972**, *34*, C9.

stirrer, an inside thermometer, and a dry ice/2-propanol reflux condenser, 44 g (113.4 mmol) of $B[C_2H_4SiHCl_2]_3\}_n$[16a] was dissolved in 1.5 L of tetrahydrofuran and cooled to 0 °C. Under vigorous stirring, a moderate stream of ammonia was introduced to the solution whereby ammonium chloride precipitation was immediately observed. During the reaction, the temperature of the mixture did not rise above 10 °C. The addition of ammonia was continued, until liquid ammonia condensed at the reflux condenser (∼40 min). After the addition of ammonia was completed, the reaction mixture was allowed to warm overnight to 25 °C and then filtered through a pad of Celite. The precipitate, containing the insoluble byproduct ammonium chloride and insoluble precursor, was thoroughly extracted two times with 100 mL of tetrahydrofuran each and then disposed. The filtrate and the extract were combined and concentrated at elevated temperature (finally 80 °C) in a high vacuum to produce 18 g (79.2 mmol, 70%) of $\{B[C_2H_4Si(H)NH]_3\}_n$ (**1***M*) as a colorless powder that is very sensitive to moisture and air. Anal. Found: C, 34.9; H, 8.1; N, 17.7; B, 4.5; Si, 32.0. $[C_6H_{18}N_3BSi_3]_n$ ([227.28]$_n$) Calcd: C, 31.71; H, 7.98; N, 18.48; B, 4.75; Si, 37.08. IR (KBr): ν(N−H) = 3359 s; ν(C−H) = 2934 s, 2895 m, 2864 s; ν(Si−H) = 2119 vs; $\delta(CH_3)$ = 1462 m; δ_s(C−C) = 1336 m; δ(Si−N−H) = 1160 vs; ν(Si−N) = 849 s, br, cm^{-1}. ^{13}C CP-MAS NMR: δ = 12.3 (*C*H$_3$), 26.8 (*C*H$_2$), 28.0 (br, sh, *C*H). ^{11}B CP-MAS NMR: δ = −1.0. ^{29}Si CP-MAS NMR: δ = −13.6. TGA (argon, 1400 °C, 88% ceramic yield): 25−250 °C, Δm = 0%; 250−750 °C, Δm = 11%; 750−1400 °C, Δm = 1%.

2.3. Synthesis of $\{B[C_2H_4Si(NH)_{1.5}]_3\}_n$ (2*M*). The synthesis of **2***M* was performed according to the procedure described above. A 24 g (480 mmol) sample of $B[C_2H_4SiCl_3]_3\}_n$[22] was dissolved in 1 L of tetrahydrofuran and reacted with ammonia. Since only less than 5% yield of the precursor could be obtained after the filtration step, spectroscopic studies as well as thermogravimetric investigations were not performed.

2.4. Synthesis of $\{B[C_2H_4Si(H)NH]_3\}_n$ (1*P*). In a 4 L Schlenk flask equipped with a 500 mL dropping funnel and a magnetic stirrer, 148.6 g (2.09 mol) of $[(H_2C{=}CH)SiHNH]_n$[20] was dissolved in 1.5 L of toluene. Under vigorous stirring, 348 mL (696 mmol) of a 2 M solution of $H_3B{\cdot}S(CH_3)_2$ in toluene was quickly added. During the slightly exothermic addition of borane dimethyl sulfide, the reaction mixture was cooled with a water bath and the temperature controlled to not rise above 25 °C. Approximately 30−120 min after the addition was finished, the viscosity of the colorless solution started to significantly increase to give a colorless rubber-like gel. After 12 h the volatile components (solvent, dimethyl sulfide) were evaporated in a high vacuum at elevated temperature (finally 130 °C) to produce 156 g (688 mmol, 100%) of $\{B[C_2H_4Si(H)NH]_3\}_n$ (**1***P*) as a colorless powder that is very sensitive to moisture and air. Anal. Found: C, 31.6; H, 7.75; N, 19.3; B, 4.55; Si, 35.9; O, 1.5. $[C_6H_{18}N_3BSi_3]_n$ ([227.28]$_n$) Calcd: C, 31.71; H, 7.98; N, 18.48; B, 4.75; Si, 37.08. IR (KBr): ν(N−H) = 3379 vs; ν(=C−H) = 3085 vw, 3049 vw, 3026 vw; ν(C−H) = 2926 vs, 2895 m, 2870 s; ν(B−H) = 2432, w; ν(Si−H) = 2128 vs; $\delta(CH_3)$ = 1463 m; δ(Si−N−H) = 1155 s, br; ν(Si−N) = 846 s, br, cm^{-1}. ^{13}C CP-MAS NMR: δ = 12.0 (*C*H$_3$), 22.7 (*C*H$_2$), 26.9 (*C*H), 130.1 (C=C), 138.2 (C=C). ^{11}B CP-MAS NMR: δ = 0. ^{29}Si CP-MAS NMR: δ = −15.6. TGA (argon, 1400 °C, 86.5% ceramic yield): 25−250 °C, Δm = 0%; 250−700, Δm = 13.5%; 700−1400 °C, Δm = 0%.

2.5. Synthesis of $\{B[C_2H_4Si(NH)_{1.5}]_3\}_n$ (2*P*). According to the synthesis of **1***P*, 88 mL of a 2 M solution of $H_3B{\cdot}S(CH_3)_2$ in toluene was rapidly added to 41 g (530 mmol) of $[(H_2C{=}CH)Si(NH)_{1.5}]_n$[21] dissolved in 1 L of toluene. After approximately one-third of the borane was added, the polymeric precursor began to precipitate from the solution as a colorless solid. After complete borane addition, stirring was continued for 2 h more. Following, all volatile components were removed in a vacuum (10^{-1} mbar, 25− 130 °C) to produce 43.5 g (176 mmol, 100%) of $\{B[C_2H_4Si(NH)_{1.5}]_3\}_n$ (**2***P*) as a colorless, very fine grained powder that is extremely sensitive to moisture and air. Anal. Found: C, 29.8; H, 6.8; N, 23.8; B, 4.5; Si, 33.6; O, 1.1. $[C_6H_{16.5}N_{4.5}BSi_3]_n$ ([246.78]$_n$) Calcd: C, 29.20; H, 6.74; N, 25.53; B, 4.38; Si, 34.15. IR (KBr): ν(N−H) = 3394 s; ν(=C−H) = 3049 w; ν(C−H) = 2942 s, 2870 m; ν(B−H) = 2477 w; ν(C=C) = 1606 vw; $\delta_{asym}(CH_3)$ = 1463 w; ν(C−C) = 1405 w; δ(Si−N−H) = 1172 vs; ν(Si−N) = 921 vs cm^{-1}. ^{13}C CP-MAS NMR: δ = 12.8 (*C*H$_3$), 28.3 (*C*H), 130.4 (C=C), 137.6 (C=C). ^{11}B CP-MAS NMR: δ = −0.5. ^{29}Si CP-MAS NMR: δ = −21.0, −33.3. TGA (argon, 1100 °C, 84% ceramic yield): 25−300 °C, Δm = 0%; 300−700 °C, Δm = 14%; 700−1100 °C, Δm = 2%.

2.6. Synthesis of $\{B[C_2H_4Si(NH)_{1.5}]_3\}_n$ (2*D*). The detailed synthesis and spectroscopic data of 2*D* are described elsewhere.[23] In a typical experiment, 20 g (106.4 mmol) of $B[C_2H_4SiH_3]_3$[24] and 0.5 mL of 2.5 M ^{n}BuLi (1.25 mmol, ∼1 mol % in *n*-hexane) were dissolved in 400 mL of toluene and heated to 75 °C. Under vigorous stirring, ammonia was slowly added whereby a clouding of the solution and the evolution of hydrogen immediately took place. After the addition of ammonia was completed, all volatile components were removed in a high vacuum (finally 120 °C, 10^{-3} mbar) to produce 24.2 g (98.1 mmol, 88%) of $\{B[C_2H_4Si(NH)_{1.5}]_3\}_n$ (**2***D*) as a colorless, fine grained powder.

2.7. Synthesis of $\{B[C_2H_4Si(CH_3)NH]_3\}_n$ (3*P*). According to the synthesis of **1***P* and **2***P*, 151 mL (302 mmol) of a 2 M solution of $H_3B{\cdot}S(CH_3)_2$ in toluene was added to 77.1 g (905 mmol) of $[(H_2C{=}CH)Si(CH_3)NH]_n$[21] dissolved in 1.5 L of toluene. In contrast to the synthesis of compounds **1***P* and **2***P*, a direct precipitation of the polymer from the solution was not observed. When the addition of borane dimethyl sulfide was completed, stirring was continued until the next day. Finally, all volatile components were removed in a vacuum (10^{-3} mbar, 25−130 °C) to produce 77.5 g (288 mmol, 95%) of $\{B[C_2H_4Si(CH_3)NH]_3\}$ (**3***P*) as a colorless powder that is very sensitive to moisture and air. Anal. Found: C, 40.6; H, 8.6; N, 14.8; B, 3.9; Si, 30.9; O, 1.1. $[C_9H_{24}N_3BSi_3]_n$ ([269.38]$_n$) Calcd: C, 40.13; H, 8.98; N, 15.60; B, 4.01; Si, 31.28. IR (KBr): ν(N−H) = 3402 s; ν(C−H) = 2954 s, 2919 m, 2868 s; $\delta_{asym}(^CCH_3)$ = 1459 w; $\delta_{sym}(^CCH_3)$ = 1405 m; $\delta_{sym}(^{Si}CH_3)$ = 1255 s; δ(Si−N−H) = 1164 vs; ν(Si−N) = 915 vs cm^{-1}. ^{13}C CP-MAS NMR: δ = 2.3 (Si*C*H$_3$), 12.3 (CH*C*H$_3$), 30.1 (*C*HCH$_3$). ^{11}B CP-MAS NMR: δ = 6.0. ^{29}Si CP-MAS NMR: δ = −4.5, −1.8. TGA (1100 °C, 55% ceramic yield): 180−700 °C, Δm = 45%.

3. Results and Discussion

3.1. Synthesis. Boron-modified polysilazanes of the type $\{B[C_2H_4Si(R)NH]_3\}_n$ [**1**, R = H; **2**, R = $(NH)_{0.5}$] were obtained by several different methods. The first method was by ammonolysis of monomeric tris(chlorosilylethyl)-boranes $B[C_2H_4Si(R)Cl_2]_3$ (Scheme 1; monomer route, index *M*; R = H, Cl, CH$_3$[6,12]). The boranes themselves were described previously and obtained by hydroborating the corresponding vinylchlorosilanes $(H_2C{=}CH)Si(R)Cl_2$ with borane dimethyl sulfide, $BH_3{\cdot}S(CH_3)_2$.[16a,22]

The starting compounds $B[C_2H_4Si(R)Cl_2]_3$ were dissolved in tetrahydrofuran and reacted with excess ammonia at 0 °C. The formation of large quantities of solid byproduct ammonium chloride necessitates vigorous stirring of the reaction mixture. The precursors were purified by filtration followed by vacuum evaporation of all volatile compounds at 80 °C. In the case of the hydrogen-substituted derivative **1***M*, the product was obtained as a colorless solid in only 70% yield due to its poor solubility. The synthesis of large quantities of the more highly cross-linked silsesquiazane **2***M* using this particular synthetic pathway was not possible. It was obtained in less than 5% yield after the filtration step. Because **2***M* is almost insoluble in all organic solvents, the byproduct ammonium chloride was removed by using liquid ammonia followed by filtration through a

(23) (a) Weinmann, M.; Aldinger, F. To be published. (b) Weinmann, M.; Bill, J.; Aldinger, F. Ger. Offen. DE 19741459A1, 1999.

Scheme 1. Synthesis of Polymers $\{B[C_2H_4Si(R)NH]_3\}_n$ (1−3) Using Different Reaction Pathways[a]

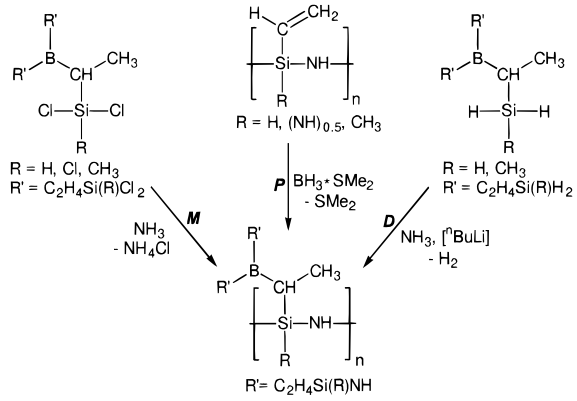

	1	2	3
	R = H	R = $(NH)_{0.5}$	R = CH_3
M	70%	>5%	80-85% [6]
P	100%	100%	95%
D	- -	88% [23]	78% [23]

[a] *M* = monomer route, *P* = polymer route, *D* = deydrogenative coupling. The table gives the product yields.

glass filter system. However, this procedure was quite difficult, requiring repeated extractions. The insoluble product always contained chloride impurities, as was determined by elemental analysis.

Compounds **1**−**3** were also obtained by hydroborating the appropriate vinyl-substituted polysilazanes $[(H_2C{=}CH)Si(R)NH]_n$ [R = H, $(NH)_{0.5}$, CH_3] using borane dimethyl sulfide in toluene (Scheme 1; polymer route, index *P*). The starting compounds themselves are accessible in high yields by ammonolysis of the respective chlorosilanes $(H_2C{=}CH)Si(R)Cl_2$ (R = H, Cl, CH_3).[20,21] Hydroboration was performed by dropwise adding borane dimethyl sulfide to a solution of the polysilazane in toluene. While the highly cross-linked precursor $\{B[C_2H_4Si(NH)_{1.5}]_3\}_n$ (**2***P*) precipitated from the reaction during borane addition, the hydrogen-substituted derivative **1***P* precipitated a couple of hours after the borane addition was finished. In contrast, the methyl-substituted derivative **3***P* remained dissolved, due to its increased solubility compared with **1***P* and **2***P*. The workup of the Si−B−C−N precursor obtained in this way was uncomplicated and required only removing all volatile components by vacuum evaporation.

A novel method of synthesizing boron-modified polysilazanes is via dehydrogenative coupling of tris(hydridosilylethyl)boranes, $B[C_2H_4Si(R)H_2]_3$ (Scheme 1; dehydrogenative coupling, index *D;* R = H, CH_3) with ammonia in the presence of suitable catalysts.[23,24] This is according to methods described previously by Seyferth et al.[8b,25] and Blum and Laine et al.[26] who reported potassium hydride- and transition metal-catalyzed cross-linking of polysilazanes by dehydrogenative Si−N coupling. The tris(hydridosilylethyl)boranes were polymerized by being dissolved in toluene and reacted with ammonia at 50−70 °C in the presence of catalytic amounts of *n*-butyllithium. Additional details will be published subsequently.[23]

3.2. Chemical Analysis and Spectroscopy. The novel precursors $\{B[C_2H_4Si(R)NH]_3\}_n$ [**1**, R = H; **2**, R = $(NH)_{0.5}$; **3**, R = CH_3] are colorless solids (**1**, **2**) or waxes (**3**), which are poorly soluble in common organic solvents (R = H, CH_3) or almost insoluble [R = $(NH)_{0.5}$]. They were characterized by FT-IR, solid-state NMR spectroscopy, and elemental analysis. The ideal (calculated) and found formulas (details in the Experimental Section) of the preceramic materials are presented in Table 1. Due to the poor solubility, molecular weights could not be determined.

A comparison of the ideal and found formulas indicates that the syntheses of precursors via the monomer *M* and the polymer *P* routes occurred in the expected manner. Since the nitrogen content in **2***D* is too low, it can be concluded that the dehydrogenative coupling did not occur quantitatively under the conditions used.[23]

The IR spectra of hydrogen-substituted **1***M* and **1***P* are very similar. They show the expected strong and broad absorption signals for the N−H stretching at 3379 cm^{-1} (**1***M*) and 3359 cm^{-1} (**1***P*). Aliphatic C−H vibrations are observed in the 2864−2934 cm^{-1} range. In addition, a set of very weak absorptions in the spectrum of **1***P*, observed at 3085, 3049, and 3026 cm^{-1}, indicates the presence of C=*C*−*H* vibrations. These moieties were not hydroborated due to the heterogeneous reaction conditions, caused by the polymer precipitating from the solution. The most remarkable features in the IR spectra of **1***M* and **1***P* are very strong ν(Si−H) bands at 2119 and 2128 cm^{-1}, respectively. The Si_2NH moieties of the polysilazane skeletons are observed as broad, very strong bands at 1160 cm^{-1} (**1***M*) and 1165 cm^{-1} (**1***P*) due to the Si−N−H deformations and at 849 cm^{-1} (**1***M*) and 846 cm^{-1} (**1***P*) due to ν(Si−N). The more highly cross-linked precursor **2***P* also shows very strong ν(N−H) bands at 3394 cm^{-1}. Bands for Si_2NH moieties in **2***P* are found at 1170 cm^{-1} [δ(Si−N−H)] and 919 cm^{-1} [ν(Si−N)]. As observed in spectra of **1***P*, residual C= *C*−*H* vibrations appear in spectra of **2***P*.

Multinuclear solid-state NMR spectroscopy represents an ideal tool for the determination of the molecular structures of preceramic polymers. ^{29}Si and ^{13}C CP-MAS NMR experiments were used to characterize compounds **1**−**3**. ^{11}B MAS NMR spectra were also obtained but gave only one broad signal without fine structure at ∼0 ppm. This value points to a 4-fold coordination of the boron centers in the solid state of **1**−**3**.

During the synthesis of the precursors via route *M*, a defined monomer is transformed into a polymer wherein the silicon environment is significantly modified. Consequently, the ^{29}Si NMR spectrum of **1***M* exhibits a high-field shift from +5 to −13.6 ppm. In contrast, syntheses

(24) Weinmann, M.; Kamphowe, T. W.; Fischer, F.; Aldinger, F. *J. Organomet. Chem.* **1999**, *592*, 115.

(25) (a) Seyferth, D.; Wiseman, G. H. *J. Am. Ceram. Soc.* **1984**, *67*, C-132. (b) Han, H. N.; Lindquist, D. A.; Haggerty, J. S.; Seyferth, D. *Chem. Mater.* **1992**, *4*, 705. (c) Dando, N. R.; Perrotta, A. J.; Strohmann, C.; Stewart, R. M.; Seyferth, D. *Chem. Mater.* **1993**, *5*, 1624.

(26) (a) Blum, Y. D.; Laine, R. M. *Organometallics* **1996**, *5*, 2081. (b) Laine, R. M.; Blum, Y. D.; Chow, A.; Hamlin, R.; Schwartz, K. B.; Rowecliffe, D. J. *Polym. Prepr.* **1987**, *28*, 393. (c) Youngdahl, K. A.; Laine, R. M.; Kennish, R. A.; Cronin, T. B.; Balavoine, G. G. *Mater. Res. Soc. Symp. Proc.* **1988**, *121*, 489. (d) Blum, Y. D.; Schwartz, K. B.; Crawford, E. J.; Hamlin, R. D. *Mater. Res. Soc. Symp. Proc.* **1988**, *121*, 565.

Table 1. Ideal and Found Formulas[a] of Compounds 1−3[b]

compd	ideal formula	found formula	compd	ideal formula	found formula
1*M*	$Si_3BC_6N_3H_{18}$	$Si_3B_{1.1}C_{6.5}N_{3.0}H_{20}$	**2***D*[23]	$Si_3BC_6N_{4.5}H_{16.5}$	$Si_3B_{1.0}C_{6.1}N_{2.5}H_{17}$
1*P*	$Si_3BC_6N_3H_{18}$	$Si_3B_{1.1}C_{6.2}N_{3.2}H_{18}$	**3***P*	$Si_3BC_9N_3H_{24}$	$Si_3B_{1.0}C_{9.1}N_{2.9}H_{23}$
2*P*	$Si_3BC_6N_{4.5}H_{16.5}$	$Si_3B_{1.0}C_{6.2}N_{4.3}H_{17}$			

[a] Referenced to Si_3. [b] Oxygen values <2 atom %.

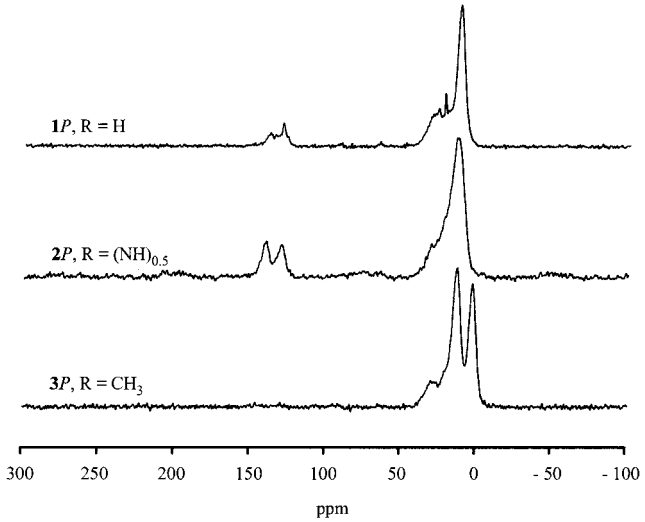

Figure 1. ^{13}C CP-MAS NMR spectra of $\{B[C_2H_4Si(R)NH]_3\}_n$ obtained by the hydroboration of the vinylated polysilazanes $[(H_2C{=}CH)Si(R)NH]_n$. Sample spinning rate 5 kHz.

of **1***P*, **2***P*, and **3***P* by hydroboration of vinyl-substituted polysilazanes $[(H_2C{=}CH)Si(R)NH]_n$ [R = H, $(NH)_{0.5}$, CH_3] with borane dimethyl sulfide are best monitored by ^{13}C CP-MAS NMR spectroscopy. With ongoing boron addition, the intensities of the olefinic carbon resonances decrease, whereas the intensities of aliphatic carbon resonances increase. A comparison of the ^{13}C NMR of compounds **1***P*−**3***P* is depicted in Figure 1.

The tendency for quantitative hydroboration increases in the order **2***P* < **1***P* < **3***P*. In the spectrum of **3***P*, olefin carbon atoms cannot be observed whereas in the spectra of **1***P* and **2***P* olefin carbon resonance signals are detectable at 130.1 and 138.2 ppm (**1***P*) and at 130.4 and 137.6 ppm (**2***P*). The aliphatic carbon atoms of the C_2H_4 units that form with hydroboration of the $H_2C{=}$CH moieties appear in the expected range at approximately 12 ppm (CH_3), 23 ppm (CH_2), and 28−30 ppm (CH). Additionally, for **3***P*, the signal at 2.3 ppm is assigned to the silicon-bonded methyl group in this polymer. A comparison by integration of the relative intensities of the olefinic and the aliphatic signals in the ^{13}C NMR spectra of **1***P* and **2***P* shows that the hydroboration occurred to only ∼95% (**1***P*) and ∼85% (**2***P*) because of poor polymer solubility, as already discussed above. In contrast, the methyl group in $\{B[C_2H_4Si(CH_3)NH]_3\}_n$ (**3***P*) provides sufficient solubility to keep the reaction homogeneous for the entire reaction period.

3.3. Thermolysis. The thermal conversion of organometallic polymers into ceramic materials is accompanied by the formation of gaseous byproducts and therefore mass loss during the polymer-to-ceramic conversion. The ceramic yields for compounds **1**−**3** were determined using thermogravimetric analysis (TGA) and the results compared with the TGA of the boron-modified polysilazane $\{B[C_2H_4Si(CH_3)NH]_3\}_n$ (T_21) described earlier by Riedel et al.[6] (Figure 2).

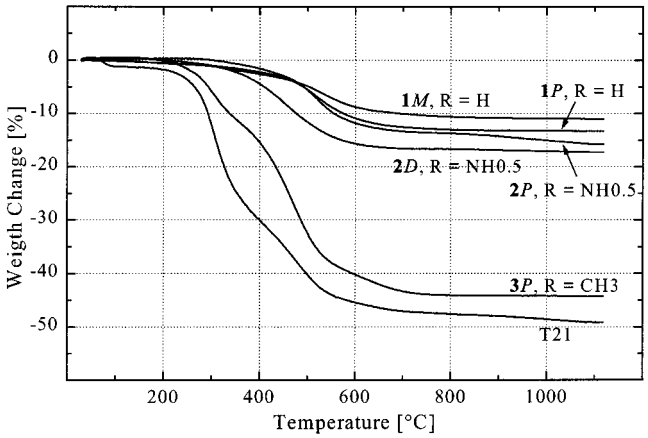

Figure 2. Thermogravimetric analysis (TGA) of $\{B[C_2H_4Si(R)NH]_3\}_n$ (**1**−**3**) and $\{B[C_2H_4Si(CH_3)NH]_3\}_n$ (T_21). Heating rate 2 °C/min; atmosphere: flowing argon.

The data in Figure 2 suggest that the substitution of the methyl units in T_21[6] with a hydrogen atom in compounds **1** significantly influences the ceramic yield. In contrast to T_21, which transforms into an amorphous Si−B−C−N material in 51% yield, the hydrogen-substituted precursors $\{B[C_2H_4SiHNH]_3\}_n$ (**1***P*, **1***M*) provide ceramic yields as high as 88% (**1***M*) and 86.5% (**1***P*). Comparable results were obtained for only a few other precursors.[8a,20b,26,27]

Mass spectra coupled with TGA of T_21 show that besides typical gaseous products such as hydrogen, hydrocarbons, and amines, low-weight oligomers also evaporate, possibly due to depolymerization of the precursor. This process, which takes place mainly in the 300−400 °C temperature range, is not observed during thermolysis of **1***M* and **1***P*, indicating their ability to further cross-link during the polymer-to-ceramic conversion process. Desirable cross-linking reactions are either *trans*-amination followed by ammonia elimination or dehydrocoupling of Si−H and N−H units with the formation of Si−N bonds (Scheme 2).[28]

A comparison of the empirical formulas of the polymeric precursors **1***M* and **1***P* and the ceramic composites obtained there from (Table 2, next section) suggests that the cross-linking occurred exclusively by dehydrocoupling, since the Si:B:N ratios at 3:1:3 are nearly identical in the polymers and the ceramics. Cross-linking by *trans*-amination, in contrast, can be excluded.

The high cross-linking of polymers **2***P* and **2***D*[23] avoids their depolymerization during the ceramization. Consequently their ceramic yields are as high as 84% and 83%, respectively (Figure 2). As already observed for **1***M* and **1***P*, the polymer-to-ceramic conversion of the isostructural polymers proceeds nearly identically, even

(27) Okamura, K.; Narisawa, M.; Iseki, T.; Oka, K.; Dohmaru, T. *Proceedings of the U.S.-Japan Joint Seminar on Future Trends in Macromolecular Hybrids*, Kyoto, Japan, 1997.
(28) Peuckert, M.; Vaahs, T.; Brück, M. *Adv. Mater.* **1990**, *2*, 1990.

Scheme 2. Cross-Linking of $\{B[C_2H_4SiHNH]_3\}_n$ (1*P*, 1*M*) by Dehydrogenative Coupling of Si−H and N−H Units (Schematic Representation)

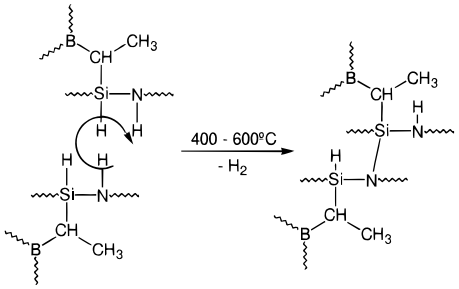

though both compounds are obtained from different reactions. Finally, a comparison of the TGA of $T_2$1 with isostructural **3***P* points out that thermolysis of these precursors also occurs similarly, even though the ceramic yield of **3***P* at 56% is somewhat higher than that of $T_2$1 (51%).

Because the polymer-to-ceramic conversion of preceramic polymers into amorphous materials is a complex process, spectroscopic analysis (solid-state NMR, IR) must be very extensive.[29,30] Thus, detailed discussion of these efforts will be published separately.[31]

3.4. High-Temperature Investigations. Ceramic materials were obtained by thermolysis of the polymers up to 1400 °C (1 °C/min) in alumina Schlenk tubes in flowing argon. The high-temperature behavior of **1***M*, **1***P*, and **2***P* ceramic materials was investigated by TGA in argon (25−2300 °C, Figure 3) and compared with the $T_2$1 material, known from the literature.[6,12] Formation of graphite/silicon carbide or graphite/silicon carbide/silicon nitride crystalline phases was monitored by X-ray diffraction (XRD; Figure 7). Microanalyses of the ceramic materials denote the empirical formulas as presented in Table 2.

A comparison of the composition of the polymers and the ceramic materials indicates that the Si:B ratio stays constant at ∼3:1 during thermolysis. Moreover, the Si:N ratio remains almost unchanged in the case of **1***M*, **1***P*, and **2***P*, whereas in the case of $T_2$1 this value is shifted from 3:2.6 to 3:2. The most apparent differences in the chemical compositions are the different carbon and nitrogen contents of the precursors and the ceramic materials. In the case of the hydrogen substituted precursor **1***M* and **1***P* the loss of only 0.9 or 1.6 carbon atoms per monomer unit is observed; **2***P* loses 3.2 carbon atoms and $T_2$1 loses 3.9 carbon atoms per monomer unit. From the ratio $M_{ceramic}$:$M_{polymer}$ it is possible to calculate the ceramic yields—provided that there is no loss of silicon-containing species during thermolysis. These ratios are 0.84 (**1***M*), 0.87 (**1***P*), 0.77 (**2***P*), and 0.70 ($T_2$1) and—except for $T_2$1—in good accordance with the findings in the TGA of the precursors (Figure 2). The deviation of 19% in the case of $T_2$1 ($M_{ceramic}$:$M_{polymer}$ × 100−51%) is, as already mentioned, due to depolymerization reactions during thermolysis and the loss of low-molecular-weight silicon- and boron-containing species.

A comparison of the high-temperature TGA of the ceramic materials (Figure 3) demonstrates a significant difference in the thermal stability of the materials obtained from **1***M*, **1***P*, and $T_2$1[6,12] and the more nitrogen rich **2***P*-derived ceramic. In contrast to the above-mentioned composites which start to decompose at temperatures around 2000 °C (**1***M*, **1***P*, 1980 °C; $T_2$1, 2050 °C[12]), the **2***P* material decomposes at 1450 °C. The latter value is comparable to that of boron-free Si−C−N ceramics that are composed of silicon nitride and free carbon.[17a,32] The mass loss of 32% in the two-step decomposition (first step 24%, second step 8%) roughly corresponds to the nitrogen content of the **2***P* material that was determined to be 28.5 mass %.

To understand the phase reactions in precursor-derived ceramics, thermodynamic calculations using the CALPHAD method (calculation of phase diagrams) were carried out.[33] In this context, phase fraction diagrams and partial pressure diagrams are very suitable for a better understanding of the manifold chemistry in higher component ceramic composites. Figure 4 shows calculated phase fraction diagrams of **1***P* and **2***P* material. The total pressure was considered to be 1 bar.

It can be concluded that the Si−B−C−N ceramic obtained from **1***P* (composition: Si, 24.0; B, 8.0; C, 44.0; N, 24.0) should, at temperatures below 1757 K, be composed of BN (16 mol %), Si_3N_4 (28 mol %), SiC (24 mol %), and 32 atom % graphite. At 1484 °C (1757 K) Si_3N_4 should react with graphite to form silicon carbide:

$$Si_3N_4 + 3C \rightarrow 3SiC + 2N_2$$

Accordingly, the total mass of the composite should decrease due to the loss of gaseous nitrogen. The amount of free carbon (graph) in this case decreases from 32.0 to 20.0 atom %, whereas the amount of silicon carbide increases from 24.0 to 48.0 mol %. However, from the high-temperature TGA investigations (Figure 3) it can be assumed that this thermodynamically expected decomposition reaction did not take place in the case of the **1***M*, **1***P*, and $T_2$1 composites. In addition, boron, which is present as boron nitride, does not thermody-

(29) (a) Burns, G. T.; Chandra, G. *J. Am. Ceram. Soc.* **1989**, *72*, 333. (b) Soraru, G. D.; Babonneau, F.; Mackenzie, J. D. *J. Mater. Sci.* **1990**, *25*, 3886. (c) Zhang, Z.-F.; Babonneau, F.; Laine, R. M.; Mu, Y.; Harrod, J. F.; Rahn, J. A. *J. Am. Ceram. Soc.* **1991**, *74*, 670. (d) Schmidt, W. R.; Interante, L. V.; Doremus, R. H.; Trout, T. K.; Marchetti, P. S.; Maciel, G. E. *Chem. Mater.* **1991**, *3*, 257. (e) Schmidt, W. R.; Marchetti, P. S.; Interante, L. V.; Hurley, W. S., Jr.; Lewis, R. H.; Doremus, R. H.; Maciel, G. E. *Chem. Mater.* **1992**, *4*, 937. (f) Laine, R. M.; Babonneau, F.; Rahn, J. A.; Zhang, Z.-F.; Youngdahl, K. A. The Effect of Monomer Architecture on Selectivity to Ceramic Products and Microstructure in Silicon Preceramic Polymers. In *Thirty Seventh Sagamore Army Materials Research Conference Proceedings*; Viechniki, D. J., Ed.; Publications Department of the Army, 1991; pp 159−169. (g) Brodie, N.; Majoral, J.-P.; Disson, J.-P. *Inorg. Chem.* **1993**, *32*, 4646. (h) Laine, R. M.; Babonneau, F.; Blowhowiak, K. Y.; Kennish, R. A.; Rahn, J. A.; Exarhos, G. J.; Waldner, K. *J. Am. Ceram. Soc.* **1995**, *78*, 137. (i) Seitz, J.; Bill, J.; Egger, N.; Aldinger, F. *J. Eur. Ceram. Soc.* **1996**, *16*, 885.

(30) (a) Schuhmacher, J.; Weinmann, M.; Bill, J.; Aldinger, F.; Müller. K. *Chem. Mater.* **1998**, *10*, 3913. (b) Schuhmacher, J.; Müller, K.; Weinmann, M.; Bill, J.; Aldinger, F. *Proceedings of the Werkstoffwoche München*, Germany; Wiley-VCH: Weinheim, 1999; p 321. (c) Müller K. In *Grain Boundary Dynamics of Precursor Derived Ceramics*; Bill, J., Wakai, F., Aldinger, F., Eds.; Wiley-VCH: Weinheim, 1999; p 197.

(31) Schuhmacher, J.; Weinmann, M.; Bill, J.; Aldinger, F.; Müller, K. To be submitted to *Chem. Mater.*

(32) Bill, J.; Seitz, J.; Thurn, G.; Dürr, J.; Canel, J.; Janos, B.; Jalowiecki, A.; Sauter, D.; Schempp, S.; Lamparter, P.; Mayer, J.; Aldinger, F. *Phys. Status Solidi* **1998**, *166*, 269.

(33) (a) Kasper, B. Ph.D. Thesis, Universität Stuttgart, 1996. (b) Seifert, H. J.; Aldinger, F. *Z. Metallkd.* **1996**, *87*, 841. (c) Seifert, H. J.; Aldinger, F. In *Grain Boundary Dynamics of Precursor Derived Ceramics*; Bill, J., Wakai, F., Aldinger, F., Eds.; Wiley-VCH: Weinheim, 1999.

Table 2. Chemical Analysis (atom %, rounded to 0.5) and Found Formula[a] of the Ceramic Materials and the Polymeric Precursor (Compare to Table 1)

compd	anal. found (atom %)[b]	ceramic formula	polymer formula
1*M*	Si 24.5, B 10.0, C 40.0, N 25.5	$Si_3B_{1.2}C_{4.9}N_{3.1}$	$Si_3B_{1.1}C_{6.5}N_{3.0}H_{20}$
1*P*	Si 24.0, B 8.0, C 44.0, N 24.0	$Si_3B_{1.1}C_{5.3}N_{3.0}$	$Si_3B_{1.1}C_{6.2}N_{3.2}H_{18}$
2*P*	Si 27.0, B 9.5, C 27.0, N 36.0	$Si_3B_{1.1}C_{3.0}N_{4.0}$	$Si_3B_{1.0}C_{6.2}N_{4.3}H_{17}$
T_21	Si 29.5, B 9.5, C 41.5, N 19.5	$Si_3B_{1.0}C_{4.3}N_{2.0.}$	$Si_3B_{1.0}C_{8.2}N_{2.6}H_{20}$

[a] Referenced to Si_3. [b] Oxygen values were determined to be <2 atom %, hydrogen <0.5 atom %.

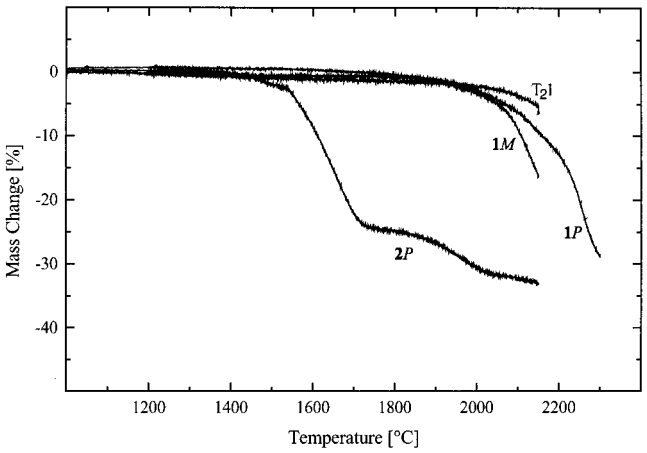

Figure 3. High-temperature TGA of the ceramic materials obtained from $\{B[C_2H_4SiHNH]_3\}_n$ (**1***M*, **1***P*), $\{B[C_2H_4Si(NH)_{1.5}]_3\}_n$ (**2***P*), and $\{B[C_2H_4Si(CH_3)NH]_3\}_n$ (T_21).[6,12,13] Heating rate (T < 1400 °C) 5 °C/min, (T > 1400 °C) 2 °C/min; argon atmosphere.

namically directly participate in any decomposition reactions below 2000 °C.

In contrast to the **1***P* composite, the **2***P* material shows the thermodynamically expected behavior (Figure 3). Calculating the different binary phase fractions for this material ($Si_3B_{1.1}C_3N_4$, Table 2) gives a composition of BN (19 mol %) Si_3N_4 (47 mol %), SiC (14 mol %), and graphite (20 atom %) (Figure 4). The most remarkable difference with the **1***P*-derived material is the Si_3N_4 value, which is 19% higher in the **2***P* ceramic. Thus, the phase amounts of SiC and C are lower, whereas the amount of BN is comparable in both composites. The decomposition of silicon nitride in the **2***P* material (reaction with C) results in 27 atom % N_2 (gas), which corresponds to 23 mass %. This is roughly the value observed in the first decomposition step in the high-temperature TGA of the **2***P* material (24 mass %, Figure 3). Due to this reaction, the amount of SiC increases to 55 mol %, whereas BN again is not involved in any reaction. Interestingly, the amount of carbon in the **2***P* material exactly corresponds to the amount of Si, which is bonded as Si_3N_4. Consequently, the material obtained due to the **2***P* decomposition should—from the thermodynamic point of view—be composed exclusively of BN and SiC.

In this context, an important detail is the dependency of the decomposition temperature of silicon nitride in the presence of graphite on the nitrogen partial pressure (Figure 5). The phase fraction diagrams in Figure 4 are calculated for 1 bar of nitrogen. Increasing the pressure from 1 to 10 bar increases the decomposition temperature from 1757 to 1973 K. Estimating a temperature of 2000 °C (2273 K), which is about the value observed for the decomposition of **1***M*, **1***P*, and T_21 in the TGA, it can be calculated that the nitrogen pressure which is

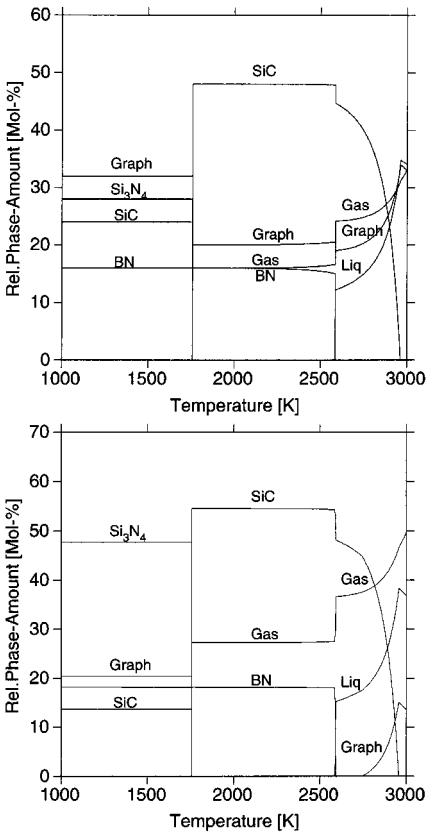

Figure 4. Calculated Si−B−C−N phase fraction diagram (p_{tot} = 1 bar) for **1***P* (Si, 24.0; B, 8.0; C, 44.0; N, 24.0; top) and **2***P* (Si, 27.0; B, 9.5; C, 27.0; N, 36.0; bottom) (atom %). In both cases reaction of Si_3N_4 and graphite at 1484 °C (1757 K) results in the formation of SiC and N_2 (gas).

necessary to inhibit the reaction of Si_3N_4 with C must be in the range of >100 bar.

Likewise, there is also degradation of silicon nitride into the elements, even though this occurs at higher temperature. The reaction temperature also strongly depends on the nitrogen partial pressure (Figure 6). Calculating 10^{-4} bar (due to the use of highly purified argon and the flowing atmosphere in all TGA experiments, the real value is probably lower) silicon nitride-containing ceramics should decompose at 1299 °C (1572 K) even without free carbon. In addition, a decomposition temperature of 2000 °C would correspond to 8 bar.

A possible hint for explaining the extraordinary high-temperature stability of precursor-derived Si−B−C−N ceramics comes from work by Jalowiecki[34] and Seifert.[35] Jalowiecki et al. investigated boron-doped silicon car-

(34) (a) Jalowiecki, A.; Bill, J.; Aldinger, F.; Mayer, J. *Composites* **1996**, *27A*, 717. (b) Jalowiecki, A. Ph.D. Thesis, Universität Stuttgart, **1997** (in German). (c) Jalowiecki, A.; Bill, J.; Mayer, J.; Aldinger, F. *Proceedings of the Werkstoffwoche München*, Germany, 1996; p 657.

(35) (a) Seifert, H. J.; Lukas, H.-L.; Aldinger, F. *Ber. Bunsen-Ges. Phys. Chem.* **1998**, *102*, 1309. (b) Seifert, H. J.; Peng, J.; Aldinger, F. *Proceedings of the Werkstoffwoche München*, Germany, 1998; in press.

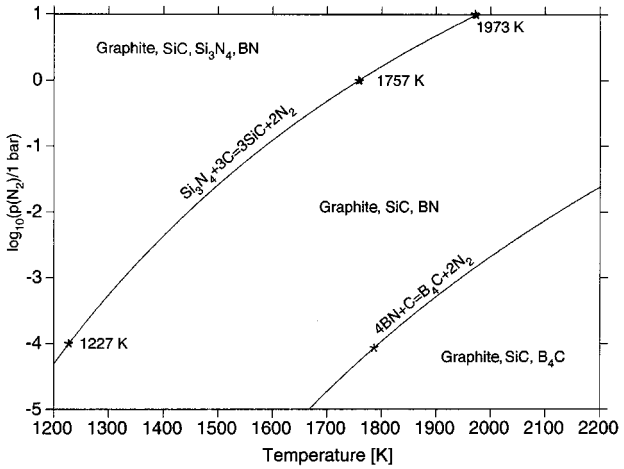

Figure 5. Partial pressure diagram for C/SiC/Si_3N_4/BN (calculated for **1***M* and **1***P* composites). Of major interest is the dependency of the decomposition temperature of Si_3N_4 and C to produce SiC and N_2. At $p(N_2) = 1$ bar this temperature is 1484 °C (1757 K), whereas at $p(N_2) = 10$ bar this value is shifted to 1700 °C (1973 K). Assuming 10^{-4} bar in argon atmosphere, the decomposition of such a composite material should occur at 954 °C (1227 K).

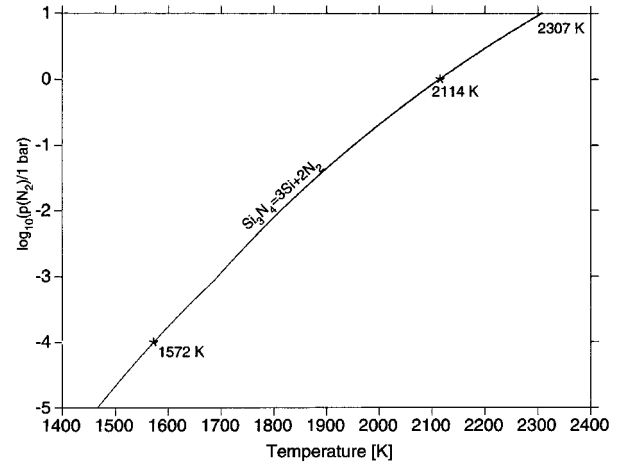

Figure 6. $\log(p(N_2))-T$ diagram for Si_3N_4. At $p(N_2) = 1$ bar Si_3N_4 decomposes at 1841 °C (2114 K) to Si(l) and N_2.[34] At $p(N_2) = 10$ bar this value is 2034 °C (2307 K). Assuming a N_2 partial pressure of 10^{-4} bar in argon atmosphere, the decomposition of Si_3N_4 should occur at 1299 °C (1572 K).

bonitride composites by HR-TEM and found turbostratic BN(C) segregation along grain boundaries of nanosized silicon carbide and silicon nitride crystals. The turbostratic BN can bind free carbon, thus decreasing its (re)-activity and inhibiting reaction with silicon nitride. Additionally, the BN(C) grain boundaries possibly serve as diffusion barriers. We suppose that, due to encapsulation of nanocrystalline silicon nitride grains by the BN(C) phase, the internal nitrogen pressure increases significantly, thus raising the decomposition temperature for the reaction of silicon nitride into the elements to unexpectedly high values.[33,35] Taking these facts into consideration, the different thermal stabilities of the **1***M*, **1***P*, and T_21[6,12] materials on one hand and the **2***P* composite on the other hand can be understood. As a consequence of the significantly increased Si_3N_4:BN ratio in the **2***P* material as compared to the **1***M*, **1***P*, and $T_2$1 materials a "protective encapsulation" of silicon nitride by turbostratic BN(C) segregations is obviously not possible.

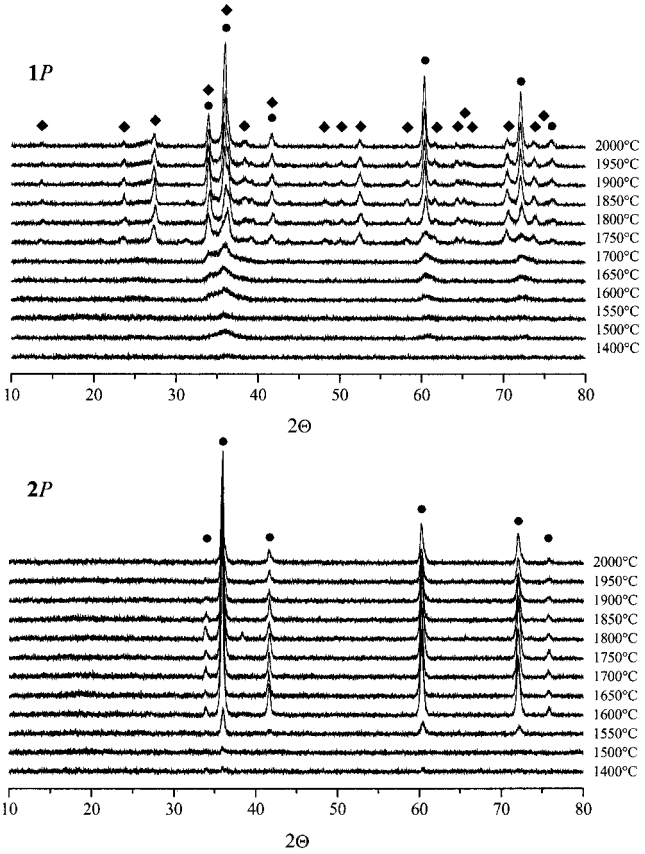

Figure 7. XRD patterns of the ceramics obtained from **1***P* (top) and **2***P* (bottom) annealed at 1400 and 1500−2000 °C (50 °C steps, 1 bar of nitrogen) for 3 h each. In the case of the **1***P* materials α/β-SiC (●) and β-Si_3N_4 (◆) reflexes are observed, whereas in the case of the **2***P* ceramic only α/β-SiC (●) reflexes are found.

The temperature-induced microstructural evolution was followed by XRD (**1***P*, **2***P*; Figure 7). In these experiments, ceramic powders were annealed in a graphite furnace (graphite crucibles, 1013 mbar nitrogen atmosphere; heating rate (T < 1400 °C) 10 °C/min, (T > 1400 °C) 2 °C/min) at 1400 and 1500−2000 °C (50 °C steps) for 3 h each.

The high-temperature TGA data (Figure 3) are nicely reflected in the crystallization experiments of **1***P* and **2***P* (Figure 7). The more nitrogen-rich **2***P* composite, which decomposes in the HT-TGA between 1500 and 1550 °C, also crystallizes at this temperature. In contrast, the **1***P* composite which decomposed at ∼2000 °C starts to crystallize between 1700 and 1750 °C. Besides the different crystallization temperatures of **1***P* and **2***P*, the most noticeable difference in the XRD patterns is the appearance of β-silicon nitride reflections in the case of the **1***P* material. In contrast, these reflections are not observed for the **2***P* composite, in accord with thermodynamic calculations (Figures 4 and 5). Moreover, it is remarkable that the intensity of the silicon nitride reflections in the **1***P* patterns does not decrease below 1950 °C! However, in both composites, the most intensive reflections arise from crystalline silicon carbide with intensities that do not decrease due to any decomposition reaction below 2000 °C. Remarkably, in the XRD patterns of **1***P*-derived material the hexagonal 6H (α-SiC) polytype is observed, whereas the XRD patterns of the **2***P* composite might allow the

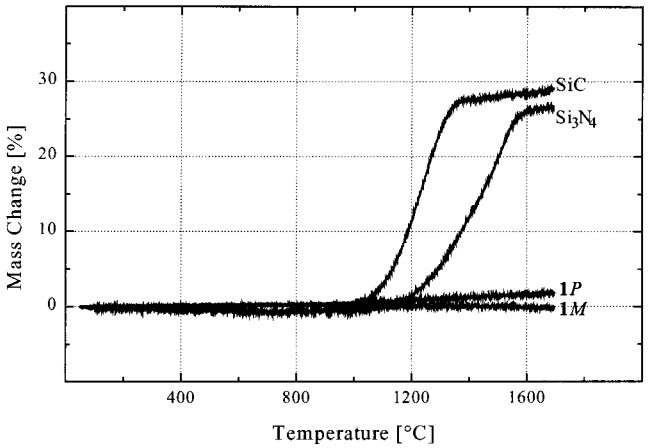

Figure 8. Oxidation behavior (TGA) of SiC, Si_3N_4, and $\{B[C_2H_4SiHNH]_3\}_n$ (**1***M*, **1***P*) ceramics. Heating rate 5 °C/min; flowing air.

conclusion that due to the decreasing intensity of the 101 and the 103 reflections with increasing temperature a 6H (α-SiC) → 3C (*β*-SiC) reverse polytype transformation occurred. Such unusual transformations were observed for α-SiC samples that were annealed in high nitrogen pressure.[36] Even more likely is the influence of texture effects which can cause a suppression of the 101 and 103 reflections.

Generally, one of the more noticeable disadvantages of non-oxide ceramics compared to oxide ceramics is their low resistance toward oxidative attack.[37] For this reason we investigated the oxidation behavior of the as-obtained **1***M* and **1***P* ceramic powders by TGA in air up to 1700 °C and compared it with those of SiC[38] and Si_3N_4 (Figure 8).[39]

In contrast to pure silicon carbide[38] and silicon nitride,[39,40] which oxidize at 1000 and 1130 °C there is—even at 1700 °C—no mass change detectable in the case of the material obtained from **1***M*, whereas there is a slight weight increase in the case of the **1***P*-derived material. This suggests either that active and passive oxidation occur simultaneously or that a thin and dense oxide layer forms, protecting the ceramic samples from further oxidation. The possible explanation for the remarkable resistance of the Si−B−C−N materials toward oxidation at elevated temperature can be concluded from scanning electron micrographs (SEM; Figures 9 and 10) for both the surface areas and a fracture surface of oxidized **1***M* ceramic particles.

The SEM investigations of the oxidized exterior of the **1***M* ceramic particles (Figure 9) illustrate that the surface areas are smooth and pore-free. Sintering of the ceramic particles, whose average grain size is 100 μm, did not occur. Fracture surfaces of the ceramic grains (Figure 10) point out that a thin layer formed during oxidation. The thickness of this pore- and crack-free layer is 1.2−2.3 μm. Bubble formation due to decomposition of native oxides as described by Nickel et al. is not observed.[41]

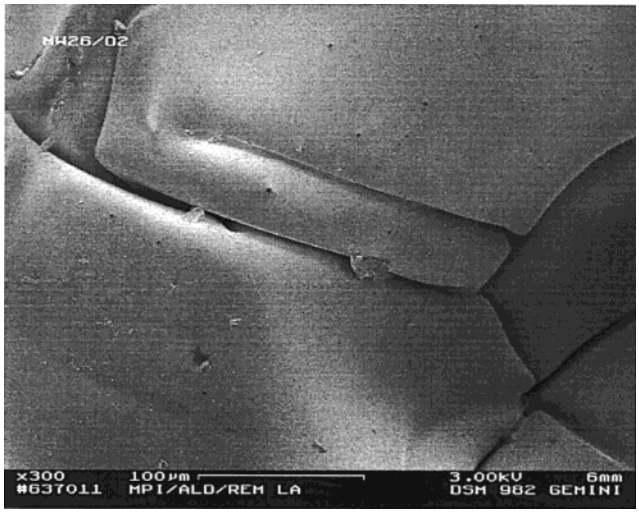

Figure 9. SEM image of surface areas of oxidized **1***M* ceramic grains (magnification 300×, reproduced at 66% of original size).

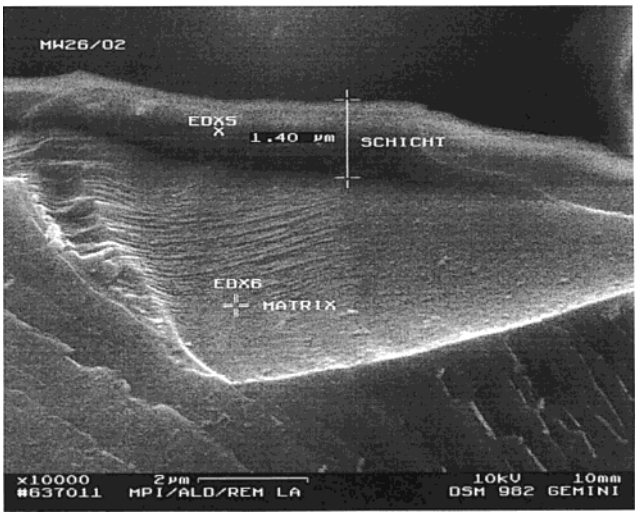

Figure 10. SEM image of a fracture surface of oxidized **1***M* material (magnification 10000×, reproduced at 66% of original size). EDX5 and EDX6 represent EDX investigated areas (see Figure 11).

EDX investigations (Figure 11) were performed to determine the chemical composition of the ceramic matrix and the layer that forms during oxidation. The results suggest that oxidation of the Si−B−C−N ceramic grains occurred exclusively at their surfaces. In contrast to the matrix, which is composed of silicon, carbon, nitrogen, and boron, the surface layer consists mainly of silicon and oxygen. Additionally, carbon can be detected in the oxide layer, but at levels lower than in the matrix. In contrast, neither nitrogen nor boron is found.

Obviously, oxidative attack causes the following reactions: silicon nitride reacts with oxygen to form silica and nitrogen. Free carbon is oxidized to carbon monoxide. Boron nitride is transformed into boron oxides and nitrogen. Boron oxides then evaporate at temperatures

(36) Kieffer, A. R.; Ettmayer, P.; Angel, E.; Schmidt, A. *Mater. Res. Bull.* **1969**, *4*, 153.
(37) Gogotsi, Y. G.; Lavrenko, V. A. *Corrosion of High-Performance Ceramics*; Springer-Verlag: Berlin, Heidelberg, 1992.
(38) ASC-26, Performance Ceramics Co., Peninsula, OH.
(39) XU 35556, Dow Corning Co., Midland, MI.
(40) For investigations on the oxidation of CVD-Si_3N_4 see for example: (a) Hirai, T.; Niihara, K.; Goto. T. *J. Am. Ceram. Soc.* **1980**, *63*, 419. (b) Narushima, T.; Ray, Y. L.; Yasutaka, I.; Hirai, T. *J. Am. Ceram. Soc.* **1993**, *76*, 1047.
(41) (a) Butchereit, E.; Nickel, K. G.; Sauer, E.; Schwab, K. *Proceedings of the Werkstoffwoche München*, Germany, 1996; p 569. (b) Butchereit, E.; Nickel, K. G. *Key Eng. Mater.* **1997**, *132−136*, 1592.

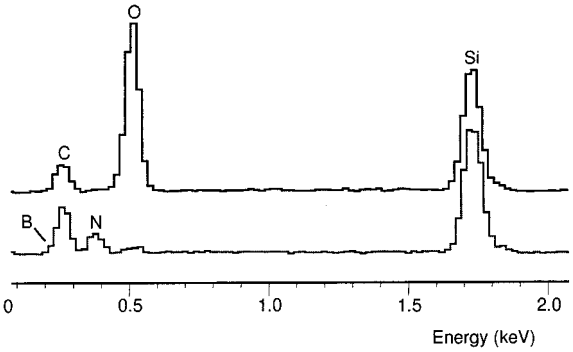

Figure 11. EDX of the fracture surface of an oxidized ceramic sample obtained from **1***M* (top, surface area EDX5; bottom, matrix EDX6; compare Figure 10).

above 1200 °C.[37] Consequently, only silica and some carbon—presumably bonded as silicon oxycarbide—remain in the oxidized layer. Comparable results were reported by Baldus and Jansen who observed by SNMS (secondary neutral particle mass spectroscopy) that oxidized surface areas of Si−B−C−N ceramics were composed of silicon, oxygen, and carbon, but free of nitrogen and boron.[3,11c] These investigations as well as our observations point to the fact that a total oxidation of Si−B−C−N composites does not occur to 1750 °C because a passivating oxide layer forms, hindering diffusion-controlled oxidation in Si−B−C−N precursor-derived ceramic composites.

Conclusions

The substitution of bulky substituents R (R = alkyl, aryl) in Si−B−C−N preceramic polymers of type $\{B[C_2H_4Si(R)NH]_3\}_n$ with low-weight entities and/or reactive moieties [R = H, $(NH)_{0.5}$] results in significantly increased ceramic yields during the polymer-to-ceramic conversion. The reaction pathway used for the synthesis of the preceramic polymers does not essentially influence the ceramization progress or the high-temperature stability of the as-obtained materials. In contrast, the chemical composition of the organometallic polymers with respect to the type and cross-linking of the polymer backbone and the type of functional groups that are bonded to the polymer skeleton play an important role. Investigations of the high-temperature stability of Si−B−C−N composites combined with thermodynamic calculations reveal that substantial amounts of silicon nitride negatively influence the high-temperature stability of these materials due to decomposition into nitrogen and silicon carbide (reaction with free carbon) or into the elements. The combination of XRD and TGA points to the fact that the decomposition reactions are accompanied by crystallization of the residual material. Only silicon-containing crystalline phases are found in our experiments. No evidence is seen for the formation of boron-containing crystalline phases. High-temperature TGA of the Si−B−C−N ceramics up to 1700 °C in air demonstrates that there is no remarkable mass change due to active or passive oxidation. As can be concluded from SEM and EDX investigations, a thin dense layer that is mainly composed of silica as well as some carbon efficiently protects the Si−B−C−N matrix from total oxidation.

Acknowledgment. We thank the Deutsche Forschungsgemeinschaft (DFG), the Fonds der Chemischen Industrie Frankfurt, and the Japan Science and Technology Corp. (JST) for financial support. We are very grateful to Dr. Georg Rixecker and Professor Richard Laine (University of Michigan) for many helpful discussions. Additionally we thank Sabine Katz for supporting us in the TGA investigations and Martina Thomas for performing the XRD studies. Hartmut Labitzke is acknowledged for his help in the SEM and EDX investigations and Gerhard Kaiser for carrying out the elemental analysis.

CM9910299